Proteolytic Action of GlpG, a Rhomboid Protease in the *Escherichia coli* Cytoplasmic Membrane†

Saki Maegawa, Koreaki Ito, and Yoshinori Akiyama*

Institute for Virus Research, Kyoto University, Kyoto 606-8507, Japan

Received July 13, 2005; Revised Manuscript Received August 25, 2005

ABSTRACT: We characterized *Escherichia coli* GlpG as a membrane-embedded protease and a possible player in the regulated intramembrane proteolysis in this organism. From the sequence features, it belongs to the widely conserved rhomboid family of membrane proteases. We verified the expected topology of GlpG, and it traverses the membrane six times. A model protein having an N-terminal and periplasmically localized β-lactamase (Bla) domain, a LacY-derived transmembrane region, and a cytosolic maltose binding protein (MBP) mature domain was found to be GlpG-dependently cleaved in vivo. This proteolytic reaction was reproduced in vitro using purified GlpG and purified model substrate protein, and the cleavage was shown to occur between Ser and Asp in a region of high local hydrophilicity, which might be located in a juxtamembrane rather than an intramembrane position. The conserved Ser and His residues of GlpG were essential for the proteolytic activities. Our results using several variant forms of the model protein suggest that GlpG recognizes features of the transmembrane regions of substrates. These results point to a detailed molecular mechanism and cellular analysis of this interesting class of membrane-embedded proteases.

Recent studies revealed the ubiquitous existence of membrane-embedded proteases in different organisms. Their biological importance has been a subject of extensive recent studies. For example, many of them have been shown to be involved in regulated intramembrane proteolysis (RIP), in which a membrane-bound precursor protein is subject to cleavage within its transmembrane region, leading to a release of a functional soluble domain from the membrane (*1*, *2*). This mode of proteolytic events is important for cellular regulation, in particular, transmembrane signaling (*1*, *2*).

RIP protease families include S2P, presenilin, signal peptide peptidase (SPP), and rhomboid. S2P proteases are zinc-activated, and those in mammals function in the ER stress responses and lipid metabolism (*1*, *2*). Bacterial S2P homologues are involved in extracytoplasmic stress response, sporulation, and differentiation (*1*, *2*). Presenilin and SPP are aspartyl proteases, involved in neuropathogenic and developmental processes and cleavage of signal peptide and viral polyproteins, respectively (*1*, *2*).

Rhomboid proteins share a few functionally essential residues, including serine, that could constitute a serine-protease catalytic active site (*3*, *4*). Rhomboids constitute one of the most widespread families of membrane proteins in the biological kingdoms (*5*). The *Drosophila* rhomboid proteins, the best characterized among this family, are involved in the release of ligands for the epidermal growth factor receptor (EGFR)[1] through proteolytic processing of their membrane-bound precursor forms such as Spitz and Gurken (*6*). The resulting EGFR ligands are essential for development of this organism. Mitochondrial rhomboid proteins in human and yeast are involved in fusion and/or remodeling of this organelle (*7*, *8*). AarA, a rhomboid homologue in a pathogenic Gram-negative bacterium *Providencia stuartii*, is suggested to have a role in the release of a signal molecule acting in quorum sensing, although its exact substrate remains unknown (*9*). *P. stuartii* AarA and *Drosphila* rhomboid-1 can function interchangeably in the respective organisms (*10*). Moreover, rhomboid proteins from diverse organisms can cleave the *Drosophila* EGFR ligand precursors in cultured cells (*4*). Recognition of Spitz by rhomboid-1 depends on a short sequence designated the "substrate motif" in a membrane−extracytoplasmic space boundary region of the Spitz transmembrane segment (*11*). It was suggested that other rhomboid proteins can recognize the same substrate motif (*11*), and that the function of rhomboid proteins is conserved across different species.

Escherichia coli produces a member of the rhomboid family, GlpG. GlpG promotes the cleavage of EGFR ligand precursors, including Spitz, when expressed in cultured mammalian cells (*4*). Although proteolytic activities have recently been demonstrated for GlpG and some other rhomboid proteins after their purification (*12*, *13*), GlpG has

† This work was supported by CREST, Japan Science and Technology Agency (to K.I.), grants from the Japan Society for the Promotion of Science (to Y.A. and K.I.), the Ministry of Education, Culture, Sports, Science and Technology, Japan (to K.I.), and the National Project on Protein Structural and Functional Analyses of the Ministry of Education, Culture, Sports, Science and Technology, Japan (to K.I.).

* To whom correspondence should be addressed: Institute for Virus Research, Kyoto University, Kyoto 606-8507, Japan. Telephone: 81-75-751-4040. Fax: 81-75-771-5699. E-mail: yakiyama@virus.kyoto-u.ac.jp.

[1] Abbreviations: EGFR, epidermal growth factor receptor; Bla, β-lactamase; CBB, Coomassie brilliant blue; DDM, *n*-dodecyl β-D-maltoside; NTA, nitrilotriacetic acid; MBP, maltose-binding protein; TM, transmembrane.

10.1021/bi051363k CCC: $30.25
Published on Web 09/24/2005

Table 1: *E. coli* Strains Used in This Study

strain	relevant genotype	ref or source
AD16	Δ*pro-lac thi*/F′ *lacI*^{q} *ZM15 Y*$^+$ *pro*$^+$	*25*
MC4100	*araD139* Δ(*argF-lac*)*U169 rpsL150 relA1* flbB5301 deoC1 ptsF25 rbsR	*26*
CU141	MC4100/F′*lacI*^{q}	*27*
AD202	MC4100, *ompT*::*kan*	*28*
AD1735	*zad-220*::Tn*10*	*14*
AK2168	*dsbA*::*cat*	*29*
ME8430	*malE*::Tn*5*	National Institute of Genetics, Japan
GW170	CU141, *malE*::Tn*5*	this study
GW220	CU141, *glpG*::*cat*	this study
GW221	GW170, *glpG*::*cat*	this study
GW338	CU141, *glpG*::*tet*	this study
GW408	GW338, *degP41*::*kan*	this study
KS474	*degP41*::*kan*	*30*
SN140	CU141, *ompT*::*kan*	this study

Table 2: Plasmids Encoding the GlpG Derivatives and the Model Substrates

plasmid	encoded protein	ref or source
pGW1	HA-GlpG	this study
pGW5	HA-GlpG(S201A)	this study
pGW43	GlpG−Bla fusion 1	this study
pGW44	GlpG−Bla fusion 2	this study
pGW45	GlpG−Bla fusion 3	this study
pGW46	GlpG−Bla fusion 4	this study
pGW47	GlpG	this study
pGW51	GlpG−Bla fusion 5	this study
pGW52	GlpG−Bla fusion 6	this study
pGW53	GlpG−Bla fusion 7	this study
pGW55	GlpG-His_6-Myc	this study
pGW66	GlpG(S201A)-His_6-Myc	this study
pGW73	MBP−LacYTM2	this study
pGW78	Bla−LacYTM2	this study
pGW86	Bla−LacYTM2−MBP-His_6	this study
pGW88	Bla−LacYTM2−MBP-His_6	this study
pGW89	HA-GlpG	this study
pGW90	HA-GlpG(S201A)	this study
pGW93	Bla−LacYTM2−MBP-His_6-Myc	this study
pGW107	HA-GlpG(H254A)	this study
pGW110	HA-GlpG(N154A)	this study
pSTD989	Bla−LacYTM6−MBP-His_6	this study
pSTD990	Bla−SecYTM6−MBP-His_6	this study
pSTD991	Bla−SpitzTM−MBP-His_6	this study
pSTD992	Bla−L20−MBP-His_6	this study
pCH85	pBR322-based vector	*14*
pHSG398	pUC-based vector	*31*
pMPM-T1	pBR322-based vector	*32*
pMPM-T1*	pBR322-based vector	this study
pSTD689	pACYC184-based vector	*33*
pSTV28	ACYC184-based vector	Takara Shuzo
pTYE007	pUC-based vector	*34*

not been studied for its intrinsic activities that are executed in the contexts of the native *E. coli* cell. Also, physiological roles and the reaction mechanism of GlpG remain unknown. In this work, we characterized *E. coli* GlpG with respect to its proteolytic activity against a model membrane protein in vivo and in vitro and a target sequence of substrate cleavage. Our experimental system and the results that were obtained open up an avenue to our deeper understanding of rhomboid proteases.

EXPERIMENTAL PROCEDURES

Bacterial Strains and Plasmids. Strains and plasmids encoding GlpG derivative proteins and model substrates are listed in Tables 1 and 2, respectively. Strains SN140 and GW170 were constructed by transferring *ompT*::*kan* from AD202 and *malE*::Tn*5* from ME8430, respectively, into CU141 by P1 transduction. Replacement of the chromosomal *glpG* gene by the *cat* and *tet* genes was carried out by transforming a hyper-recombinogenic strain with DNA fragments amplified from chromosomal DNA of AK2168 and AD1735 using pairs of primers (TTATACTGTCCCCTTTTGTGTGGAATAAGCGACAGCAACGTCAGGAGCTAAGGAAGCTAA/GTTGTGACGTTGTGTTTGTTTCATTTATAAATCCCTGGAATTACGCCCCGCCCTGCCACT and TTATACTGTCCCCTTTTGTGTGGAATAAGCGACAGCAACGTATCAGTGATAGAGAAAAGT/GTTGTGACGTTGTGTTTGTTTCATTTATAAATCCCTGGAACTAAGCACTTGTCTCCTGTT, respectively) essentially as described previously (*14*). GW220, GW221, and GW338 were P1 transductants of CU141 and GW170 that received either *glpG*::*cat* or *glpG*::*tet*. GW408 was constructed by transferring *degP41*::*kan* from KS474 to GW338 by P1 transduction.

Plasmids encoding GlpG−Bla fusion proteins were constructed as follows. First, a *glpG* fragment was amplified from the AK2168 chromosome using primers GGGGTACCCTTGATGATGATTACCTCTTTTGC and CCCAAGCTTATTTTCGTTTTCGCGCATTG (*Kpn*I and *Hin*dIII recognition sequences, respectively, are underlined) and cloned between these sites of pCH85, yielding pGW1. Next, the *Spe*I recognition sequence was inserted by site-directed mutagenesis in front of the codons for Ala87 (for HA−GlpG fusion 1), Phe133 (fusion 2), Val165 (fusion 3), Ser193 (fusion 4), Gln220 (fusion 5), Met249 (fusion 6), or the termination codon (fusion 7) of *glpG* on pGW1. Then, the *Kpn*I−*Hin*dIII *glpG* (*Spe*I) fragments of the resulting plasmids were cloned between these sites on pSTV28. Finally, a *bla* cassette fragment (*15*) was inserted into the *Spe*I site of each plasmid. pGW47 was constructed by cloning a *Kpn*I−*Hin*dIII HA−GlpG fragment of pGW1 between these sites on pSTV28. pGW55 was constructed by cloning a *glpG* fragment amplified from the AK2168 chromosome using primers GCTCTAGATTTTGTGTGGAATAAGCGACAG and GGAATTCTTTTCGTTTTCGCGCATTGAGCG (*Xba*I and *Eco*RI recognition sequences, respectively, are underlined) between these sites on pTYE007. pGW5 and pGW66 were constructed by site-directed mutagenesis of pGW1 and pGW55, respectively, using a mutagenic primer (GGTTTGGCGGGCTTGCTGGCGTGGTGTATG). pGW86 was constructed as follows. First, a *bla*′ fragment was amplified from pCH85 using primers GGAATTCCATGAGTATTCAACATTTCCGTG and CCCAAGCTTGGGGGTACCCAATGCTTAATC (*Eco*RI and *Kpn*I−*Hin*dIII recognition sequences, respectively, are underlined) and cloned between the *Eco*RI and *Hin*dIII sites of pHSG398, yielding pGW75. Then, a DNA fragment corresponding to LacY TM2 was amplified using primers GGGGTACCCCATATCAGCAAAAGTGATACG and CCCAAGCTTGGGACTAGTTTTGCGCAGCCC (*Kpn*I and *Spe*I−*Hin*dIII recognition sequences, respectively, are underlined) and cloned between the *Kpn*I and *Hin*dIII sites on the plasmid described above. The resulting plasmid was named pGW82. Finally, a DNA fragment corresponding to MBP-His_6 was amplified from the AK2168 chromosome using primers GGACTAGTAAAATCGAAGAAGGTAAACTGG and CCCAAGCTTAATGGTGATGGTGATGGTGCTTGGTGATACGAGTCT (*Spe*I and *Hin*dIII recognition sequences, respectively,

are underlined) and cloned between the *Spe*I and *Hin*dIII sites on pGW82, yielding pGW86. pGW88 was constructed by cloning an *Eco*RI−*Hin*dIII Bla−LacYTM2−MBP-His_6 fragment of pGW86 between the same sites of pSTD689. pGW93 was constructed by ligating a DNA fragment encoding the MBP-His_6-Myc fragment that had been amplified from pGW86 using primers GGACTAGT-AAAATCGAAGAAGGTAAACTGG and CCCAAGCTT-ACAGGTCCTCTTCGGAGATCAGTTTCTGTTCTTCGC-AGATATGGTGATGGTGATGGT (*Spe*I and *Hin*dIII recognition sequences, respectively, are underlined) with *Spe*I- and *Hin*dIII-digested pGW82. For construction of pGW73, a *malE′* fragment was first amplified from the AK2168 chromosome using primers GGAATTCCATGAAAATAA-AAACAGGTGCAC and CCCAAGCTTGGGGGTACCT-TGGTGATACGA (*Eco*RI and *Kpn*I−*Hin*dIII recognition sequences, respectively, are underlined) and cloned between the *Eco*RI and *Hin*dIII sites of pHSG398. Then, a DNA fragment corresponding to the LacYTM2 region, amplified using primers GGGGTACCCCATATCAGCAAAAGT-GATACG and CCCAAGCTTATTTGCGCAGCCCGAGTT-TGT (*Kpn*I and *Hin*dIII recognition sequences, respectively, are underlined), was inserted between the *Kpn*I and *Hin*dIII sites of the plasmid described above. Finally, the *Eco*RI−*Hin*dIII MBP−LacYTM2 fragment was recloned between the same sites of pSTD689. pGW78 was constructed similarly by cloning the same PCR-amplified LacYTM2 fragment between the *Kpn*I and *Hin*dIII sites of pGW75, followed by recloning of the *Eco*RI and *Hin*dIII Bla−LacYTM2 fragment between the same sites of pSTD689. Plasmids encoding derivatives of the Bla−LacYTM2−MBP-His_6 fragment having other transmembrane regions were constructed by inserting double-stranded synthetic oligonucleotides encoding either the LacYTM6 region, the SecYTM6 region, the SpitzTM region, or 20 leucine residues flanked by HISKS and SDKLG sequences on the N- and C-terminal side between the *Kpn*I and *Spe*I sites of pGW86 (see Figure 5C). pGW89 and pGW90 were constructed by cloning a *Hin*dIII−*Eco*RI fragment of pGW1 and pGW5, respectively, into the *Sma*I site of pMPM-T1* after both ends of the fragments were converted to blunt ends by T4 DNA polymerase treatment. pMPM-T1* was constructed by digestion of pMPM-T1 with *Sal*I, treatment with T4 DNA polymerase, and religation. pGW107 and pGW110 were constructed by site-directed mutagenesis of pGW89 using mutagenic primers GGCGAACGGAGCAGCCATCGC-CGGGTTAGC and GCATATCCTCTTTGCCCTGCTCTG-GTGGTG, respectively.

Media. L medium (*16*) and M9 medium (*17*) were used. Ampicillin (50 μg/mL), chloramphenicol (10 or 20 μg/mL), kanamycin (25 μg/mL), spectinomycin (50 μg/mL), and tetracycline (12.5 or 25 μg/mL) were added for selecting transformants and transductants as well as for growing plasmid-bearing strains.

Cell Fractionation and Protease Accessibility Assay. Cells were grown in L medium containing 1 mM IPTG and 1 mM cAMP at 25 °C for 30 min, washed with 10 mM Tris-HCl (pH 8.1), and suspended in 20% sucrose and 30 mM Tris-HCl (pH 8.1). They were treated with 1 mg/mL lysozyme and 10 mM EDTA at 0 °C for 30 min and fractionated into the periplasmic and spheroplast fractions by centrifugation. The cytoplasmic and membrane fractions were prepared as the supernatant and pellet after disruption of spheroplasts by sonication and differential centrifugation (*18*). Proteinase K treatment of spheroplasts was carried out as described previously (*19*).

Topology Assay of GlpG by Reporter Fusions. To assess the ampicillin resistance of strain AD16 carrying GlpG−Bla fusion proteins, cultures were diluted appropriately with 0.9% NaCl and spotted onto L agar plates containing 1 mM IPTG, chloramphenicol, and ampicillin. Cell growth was then scored after incubation at 37 °C overnight.

Immunoblotting and Pulse−Chase Experiments. Immunoblotting using anti-Myc (AB1, Santa Cruz Biotechnology, Inc.), anti-HA (Y11, Santa Cruz Biotechnology, Inc.), anti-Bla (Chemicon International), anti-His tag [His probe (H-15), Santa Cruz Biotechnology, Inc.], anti-MBP, or anti-FtsH (*20*) was carried out as described previously (*14*). Antibody-decorated proteins were visualized using the ECL detection kit (Amersham Biosciences) and Fuji LAS1000 luminoimage analyzer.

[^{35}S]Methionine pulse−chase experiments were carried out essentially as described previously (*14*). Labeled proteins were immunoprecipitated using anti-Bla and anti-MBP antibodies, separated by 10% SDS−PAGE, and visualized with a BAS1800 phosphor image analyzer.

Protein Purification and N-Terminal Amino Acid Sequence Analysis. For purification of GlpG derivatives, SN140/pGW55 and SN140/pGW66 cells were grown at 37 °C in L medium to a mid-log phase ($\sim 2 \times 10^8$ cells/mL) and induced with 1 mM IPTG and 1 mM cAMP for 6 h. Cells were collected by centrifugation, washed with 10 mM Tris-HCl (pH 8.1), suspended in 20 mL of 10 mM Tris-HCl (pH 8.1) and 10 mM 2-mercaptoethanol, and disrupted with a French press (at 8000 psi) at 4 °C. Membranes were prepared by ultracentrifugation and solubilized with 0.5% *n*-dodecyl β-D-maltoside (DDM). After clarification of the samples by low-speed centrifugation, the hexahistidine-tagged proteins were purified by nickel−nitrilotriacetic acid (NTA) agarose column chromatography with elution with a 20 to 500 mM linear gradient of imidazole in the presence of 0.1% DDM (*19*). Protein peak fractions were combined and passed through a HiTrap desalting column equilibrated with buffer A [10 mM Tris-HCl (pH 8.1), 10% glycerol, 0.02% DDM, and 1 mM DTT]. Protein peak fractions were combined and loaded onto a HiTrap SP column, which was washed with 10 column volumes of buffer A and eluted with 20 column volumes of a 0 to 1 M linear gradient of NaCl in buffer A. Peak fractions were dialyzed extensively against buffer A and stored at −80 °C.

For purification of the Bla−LacYTM2−MBP-His_6 fusion protein, cells of GW408/pGW88 were grown in L medium containing 1 mM IPTG and 1 mM cAMP at 25 °C for 2 h. Cells were collected by centrifugation, suspended in a buffer containing 10 mM Tris-HCl (pH 8.1), 10 mM 2-mercaptoethanol, and 1× protease inhibitor cocktail (nacalai tesque). The solubilized membrane fraction was purified by Ni−NTA column chromatography as described above.

The in vivo-generated C fragment of the Bla−LacYTM2−MBP-His_6 protein in cells of AD16/pGW86 was first isolated by Ni−NTA column chromatography as described above. Then the peak fractions were combined and loaded on an amylose resin (New England Biolabs, Inc.) column, which was washed with 20 column volumes of buffer B [20 mM

Tris-HCl (pH 8.1), 200 mM NaCl, 1 mM EDTA, and 10 mM 2-mercaptoethanol], and eluted with 10 column volumes of buffer B containing 10 mM maltose. For determination of the N-terminal amino acid sequences of the GlpG cleavage product of the Bla−LacYTM2−MBP-His_6 protein, the in vivo- and in vitro-generated C fragments were blotted onto a PVDF membrane and subjected to sequencing (custom services by Shimazu Biotech).

In Vitro Protease Activity Assays. The reaction mixture for the in vitro cleavage of the Bla−LacYTM2−MBP-His_6 protein contained the wild type or a mutant form of GlpG-His_6-Myc, Bla−LacYTM2−MBP-His_6, 55 mM Tris-HCl (pH 8.1), 0.02% DDM, 7.5% glycerol, 10 mM 2-mercaptoethanol, 100 mM KCl, and 10% polyethylene glycol 3350. It was incubated at 37 °C, and portions were sampled and mixed with $^1/_5$ volume of 5× SDS sample buffer. Proteins were then separated by 10% SDS−PAGE and stained with Coomassie brilliant blue (CBB). The casein degradation activity of GlpG was assayed in the same buffer except that polyethylene glycol 3350 was omitted. Fluorescence emission at 530 nm was measured with an excitation wavelength of 490 nm, using a Hitachi F-4500 fluorometer.

RESULTS

Topology of GlpG in the E. coli Cytoplasmic Membrane. E. coli GlpG contains six hydrophobic stretches (Figure 1A). We expressed N-terminally HA-tagged GlpG and confirmed its fractionation as an integral cytoplasmic membrane protein (data not shown). We then investigated the membrane topology of GlpG by constructing a series of GlpG−Bla fusion proteins in which growing N-terminal segments of GlpG were followed by the mature Bla sequence (Figure 1A). The Bla domain can report its periplasmic localization in the increased ampicillin resistance of a host cell (*21*). We detected the fusion proteins by anti-Bla immunoblotting as proteins of increasing sizes (Figure 1B). Cells expressing fusion proteins 2, 4, and 6 resisted 50 μg/mL ampicillin, whereas those expressing fusion proteins 1, 3, 5, and 7 did not (Figure 1B, bottom panel). The accumulation levels of the fusion proteins of the latter class were no lower than those of the former. These results identified the three periplasmic regions in GlpG. We conclude that it traverses the membrane six times with its N- and C-termini facing the cytoplasm as illustrated in Figure 1C. Our topology model agrees with a recent proposal (*22*) based on computer-based topology prediction and the experimental results which show that the C-terminal GFP/PhoA tag was cytoplasmic.

Construction of a Model Substrate for GlpG. We were able to replace the chromosomal *glpG* with either the *cat* or the *tet* gene. The *glpG*-disrupted strains grew normally in rich (L) and minimal (M9) media at 30, 37, and 42 °C (data not shown). Thus, GlpG is not essential for growth under these conditions. Although we have assumed GlpG acts as a protease, this concept remained unverified when we started this study and until very recent two publications of biochemical characterization of GlpG and other rhomboid proteins (*12*, *13*). Also, no information about substrate proteins of GlpG as well as physiological roles played by GlpG in *E. coli* cells is yet available. The objective of this study was to characterize GlpG in the contexts of the *E. coli* cell. We thus constructed a model membrane protein as one

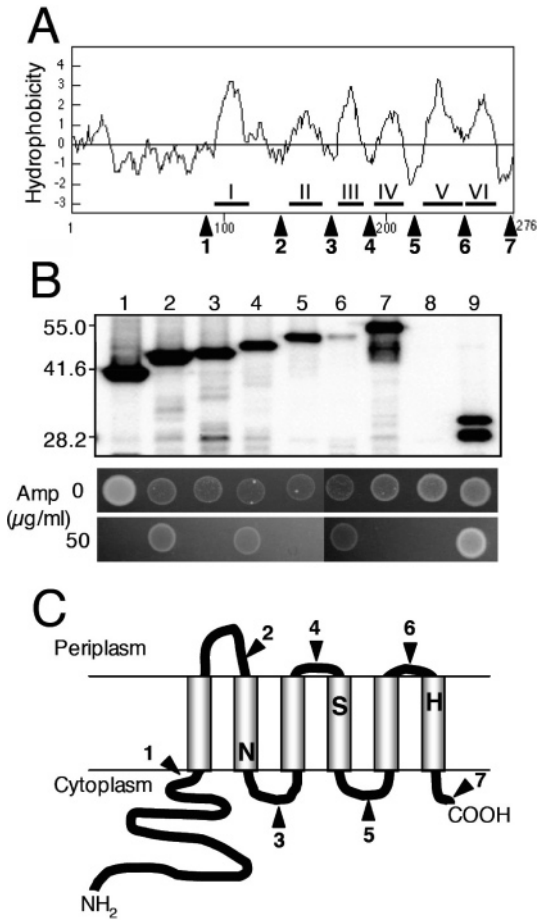

FIGURE 1: Topology of GlpG in the cytoplasmic membrane. (A) The hydropathy profile of the GlpG sequence was generated according to the method of Kyte and Doolittle (*35*) with an 11-residue window. Hydrophobic regions (I−VI) and the positions of the Bla fusions (1−7) are indicated. (B) Cellular accumulation of the GlpG−Bla fusion proteins and ampicillin resistance. In the top panel, strain AD16 was transformed with either a plasmid encoding one of the GlpG−Bla fusions (lanes 1−7 correspond to fusions 1−7, respectively), pGW47 ($GlpG^+$) (lane 8), or a combination of pGW47 and pCH85 (vector) (lane 9). The plasmid-bearing cells were grown at 37 °C in L medium and induced with 1 mM IPTG for 2 h. Proteins were precipitated with 5% trichloroacetic acid and analyzed by SDS−PAGE and immunoblotting using anti-Bla antibodies. Molecular size marker positions (kilodaltons) are shown at the left. In the bottom panels, each of the cultures used in the experiments described above was diluted with saline and a portion (containing ~3×10^4 cells) was spotted onto a set of two L-IPTG plates, one containing ampicillin (50 μg/mL) and the other not. (C) A schematic representation of the GlpG topology. The putative serine protease active site residues (Ser201, Asn154, and His254) are shown.

of our attempts to search for a GlpG substrate. It was a chimeric Bla−LacYTM2−MBP-His_6 protein that consisted of the Bla precursor sequence (including a signal sequence), the sequence around the second transmembrane region of LacY (LacYTM2), the MBP sequence, and finally a hexahistidine tag in this N-terminus to C-terminus order. This fusion protein was designed to have type I ($N_{OUT}-C_{IN}$) topology (Figure 2A) on the basis of the known property of rhomboid substrates in eukaryotic cells. We originally constructed this fusion protein as a platform for examining various transmembrane sequences by exchanging them with the LacYTM2 part and examining resulting variants whether they receive GlpG-dependent cleavage.

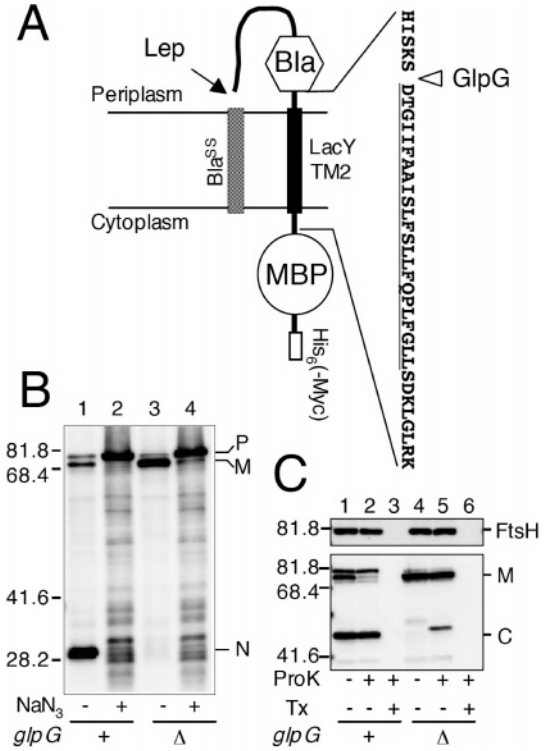

FIGURE 2: Localization and topology of the Bla−LacYTM2−MBP-His_6 model membrane protein. (A) Organization and membrane topology. Bla^{SS} and Lep indicate the signal sequence of Bla and leader peptidase, respectively. Highlighted by amino acid sequence is the LacY-derived part, in which the region predicted to be transmembrane regions by the SOSUI program (*36*) is underlined. The position of GlpG-catalyzed cleavage is indicated with an arrowhead. (B) Effects of NaN_3 on the signal sequence processing and the GlpG-dependent cleavage of the model protein. Cells of GW170 (*malE*::Tn*5*, *glpG*$^+$)/pGW88 (Bla−LacYTM2−MBP-His_6) and GW221 (*malE*::Tn*5*, *glpG*::*cat*)/pGW88 were grown at 25 °C in L medium, and 1 mM IPTG, 1 mM cAMP, and 0.02% NaN_3 were added. After 30 min, proteins were analyzed by SDS−PAGE and anti-Bla immunoblotting. (C) Cytoplasmic localization of the C-terminal region of the Bla−LacYTM2−MBP-His_6-Myc protein. Cells of GW170/pGW93 (Bla−LacYTM2−MBP-His_6-Myc) and GW221/pGW93 were grown at 25 °C in L medium and induced with 1 mM IPTG and 1 mM cAMP for 30 min. Cells were converted to spheroplasts and treated with 1 mg/mL proteinase K (ProK) in the presence or absence of 1% Triton X-100 (Tx) as indicated. Proteins were analyzed by SDS−PAGE and anti-Myc (bottom panel) and anti-FtsH (top panel) immunoblotting. FtsH, a cytoplasmic membrane protein having a protease-resistant periplasmic region and a large cytoplasmic domain, served as an internal control showing the spheroplast integrity. P and M represent the precursor (signal sequence-retaining) and mature (signal sequence-processed) forms of the model protein, respectively. N and C denote the N-terminal and C-terminal fragments of the model protein, respectively, generated by the GlpG-dependent cleavage. Molecular size marker positions (kilodaltons) are shown at the left in panels B and C.

To our surprise, the Bla−LacYTM2−MBP-His_6 protein itself proved to be cleaved by GlpG as shown below. We first verified that this artificially designed model protein indeed assumed type I topology in the membrane by expressing it in a Δ*glpG* strain. When the fusion gene on a plasmid was induced, a protein of 77 kDa was detected by anti-Bla, anti-MBP, and anti-His_6 immunoblotting (Figure 2B, lane 3). Cell fractionation experiments showed that this protein was mostly membrane-associated (data not shown). When cells were treated with 0.02% NaN_3, a protein export inhibitor, before induction, this fusion protein exhibited a retarded SDS−PAGE mobility (Figure 2B, lane 4), indicating that the N-terminal signal sequence had not been removed. It is in turn inferred that, in the absence of the inhibitor, the N-terminal region is translocated into the periplasmic side of the membrane, where the Lep (leader peptidase) active site resides. Periplasmic localization was also confirmed for the N-terminal Bla domain of the fusion protein by the formation of an intramolecular disulfide bond in it (data not shown).

We examined the localization of the C-terminal region by protease accessibility assays using spheroplasts (Figure 2C). In this particular experiment, a derivative of the model protein having a C-terminal His_6-Myc bipartite tag (Bla−LacYTM2−MBP-His_6-Myc) was used. The C-terminally attached Myc epitope was inaccessible to externally added proteinase K, whereas it was digested after solubilization of the membrane with Triton X-100 (Figure 2C, lanes 4−6). Thus, the C-terminus of the fusion protein remained inside the spheroplasts. The low-efficiency cleavage of the intact protein in spheroplasts in the experiments depicted in Figure 2C may have been due to the protease-resistant folding of the Bla domain. Taken together, we conclude that the model protein has its Bla domain on the periplasmic side and its C-terminal region, presumably the MBP domain as well, on the cytoplasmic side of the membrane.

GlpG-Dependent Cleavage of the Model Protein in Vivo. We also expressed the Bla−LacYTM2−MBP-His_6 fusion protein in wild-type cells and found that the amount of intact band observed in the Δ*glpG* cells was greatly reduced. Instead, two new bands, one containing the N-terminal Bla domain (N fragment) and the other containing the C-terminal MBP domain (C fragment), were detected in wild-type cells by respective antibodies (Figure 3A, lanes 2 and 5). Our screening of a variety of protease-deficient mutants indicated that only the Δ*glpG* mutant gave the fully abundant intact protein. We then followed the biosynthesis of this protein by pulse−chase experiments (Figure 3B). In wild-type cells, the fusion protein was labeled initially as the full-length product (Figure 3B, lanes 1 and 7), whereas increasing intensities of the N and C fragments appeared during the chase with a concomitant decrease of radioactivities associated with the full-length protein. In contrast, the Bla−LacYTM2−MBP-His_6 protein remained stable in the Δ*glpG* strain up to 10 min. To establish that the Bla−LacYTM2−MBP-His_6 protein is cleaved in a manner that is dependent on functional GlpG, we coexpressed HA-tagged GlpG as well as its variant having an alanine substitution for the possible protease active site serine (Ser201) of GlpG (see Figure 1C). When HA-GlpG was expressed in the Δ*glpG* strain, the amount of the full-length Bla−LacYTM2−MBP-His_6 product decreased remarkably while the N and C fragments were evident (Figure 3C, lanes 1 and 2). In contrast, HA-GlpG-(S201A) was ineffective in mediating the proteolytic conversion of the fusion protein into the two fragments (Figure 3C, lane 3). These results strongly suggest that GlpG indeed cleaves the fusion protein in vivo. The size of the N fragment (Figure 3A, lane 2) was almost the same as that of the mature Bla protein (lane 1), whereas the C fragment (lane 5) was slightly larger than the mature MBP protein (lane 4), suggesting that GlpG introduces a cleavage around the Bla−LacYTM2 junction of the fusion protein.

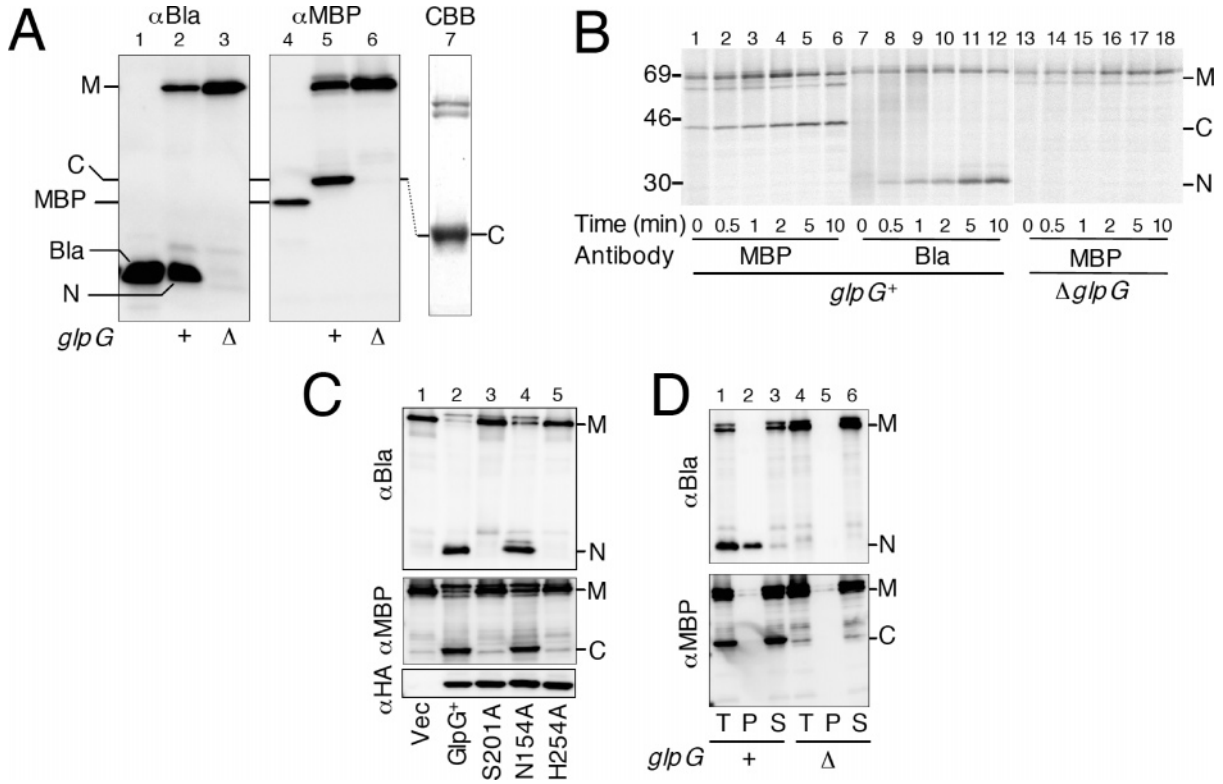

FIGURE 3: GlpG cleaves the Bla−LacYTM2−MBP-His_6 model membrane protein in vivo. (A) Cells of CU141 (*malE*$^+$)/pCH85 (Bla) (lane 1), GW170 (*malE*::Tn*5*, *glpG*$^+$)/pGW88 (Bla−LacYTM2−MBP-His_6) (lanes 2 and 5), GW221 (*malE*::Tn*5*, *glpG*::*cat*)/pGW88 (lanes 3 and 6), and CU141 (lane 4) were grown at 25 °C in L medium and exposed to 1 mM IPTG and 1 mM cAMP for 30 min. Total cellular proteins were then subjected to SDS−PAGE separation and anti-Bla (lanes 1−3) and anti-MBP (lanes 4−6) immunoblotting. Lanes 1 and 4 show mature Bla and mature MBP proteins, respectively, expressed from the respective wild-type genes. Lane 7 shows the CBB staining pattern of a preparation of the C-terminal fragment of the model protein purified from cells of AD16/pGW86 (Bla−LacYTM2−MBP-His_6) as described in Experimental Procedures. (B) Biosynthesis and cleavage of the Bla−LacYTM2−MBP-His_6 protein as followed by pulse−chase analysis. Cells of GW170/pGW88 and GW221/pGW88 were grown at 25 °C in M9-glucose (0.4%) medium supplemented with 18 amino acids (other than Met and Cys) and induced with 1 mM IPTG and 1 mM cAMP for 10 min. Cells were pulse-labeled with [^{35}S]-methionine for 1 min and chased with unlabeled methionine for the indicated periods. Labeled proteins were then immunoprecipitated with anti-MBP and anti-Bla as indicated, separated by SDS−PAGE, and visualized by BAS1800 phosphor imager. Molecular size marker positions (kilodaltons) are shown at left. (C) The cleavage of the Bla−LacYTM2−MBP-His_6 protein is mediated by the serine protease function of GlpG. The GW221/pGW88 strain was further transformed with pMPM-T1* (vector, lane 1), pGW89 (HA-GlpG$^+$, lane 2), pGW90 [HA-GlpG(S201A), lane 3], pGW110 [HA-GlpG(N154A), lane 4], and pGW107 [HA-GlpG(H254A), lane 5]. Cloned genes were induced with 1 mM IPTG and 1 mM cAMP at 25 °C for 30 min. Proteins were analyzed by SDS−PAGE and immunoblotting using either anti-Bla, anti-MBP, or anti-HA as indicated. (D) Localization of the cleavage products. Cells of GW170/pGW88 (lanes 1−3) and GW221/pGW88 (lanes 4−6) were grown in L medium at 25 °C and induced with 1 mM IPTG and 1 mM cAMP for 30 min. They were then fractionated into spheroplast (S) and periplasm (P) fractions by sucrose−lysozyme treatment. Proteins of each fraction and the whole cells (T) were analyzed by SDS−PAGE and anti-Bla (top panel) and anti-Myc (bottom panel) immunoblotting.

Upon spheroplast formation of the *glpG*$^+$ cells, the N fragment was released into the periplasmic fraction while the C fragment remained associated with the spheroplast (Figure 3D, lanes 1−3). The cytoplasmic localization of the latter fragment was shown by the proteinase K resistance of its C-terminal Myc epitope in the absence of detergent solubilization of the cytoplasmic membrane (Figure 2C, lanes 1−3). These results suggest that GlpG acts against the membrane-integrated form of the fusion protein. This was supported further by the fact that NaN_3 inhibition of membrane integration resulted in accumulation of the full-length precursor protein that received neither the Lep-dependent nor the GlpG-dependent cleavage (Figure 2B, lane 2).

Rhomboid proteins are considered to be serine proteases having a conserved Ser, Asn, and His triad required for catalysis (*3*, *4*). We examined the importance of the conserved Asn and His residues (Asn154 and His254) in GlpG (see Figure 1C) for in vivo cleavage of the model substrate. Recent studies showed that the conserved His residue is essential but Asn is dispensable for the functionality of YqgP, a *Bacillus subtilis* rhomboid ortholog (*4*, *13*). Consistent with the reports mentioned above, it was found that the proteolytic function of GlpG was lost with the His254Ala alteration but not with the Asn154Ala alteration (Figure 3C, lanes 4 and 5). Thus, among the suspected active site residues, Asn154 is not essential.

Purification and in Vitro Characterization of GlpG as a Protease. For biochemical characterization of GlpG, we purified the wild type and a S201A mutant form of GlpG-His_6-Myc as well as the model substrate protein, Bla−LacYTM2−MBP-His_6. Membranes were prepared from cells overexpressing GlpG-His_6-Myc, GlpG(S201A)-His_6-Myc, or Bla−LacYTM2−MBP-His_6 and solubilized with DDM. These proteins were then purified by Ni−NTA column chromatography. Additional cation exchange chromatography was also included for purification of GlpG.

When the Bla−LacYTM2−MBP-His_6 protein was incubated at 37 °C with GlpG-His_6-Myc, it was converted into a smaller fragment with a SDS−PAGE mobility indistin-

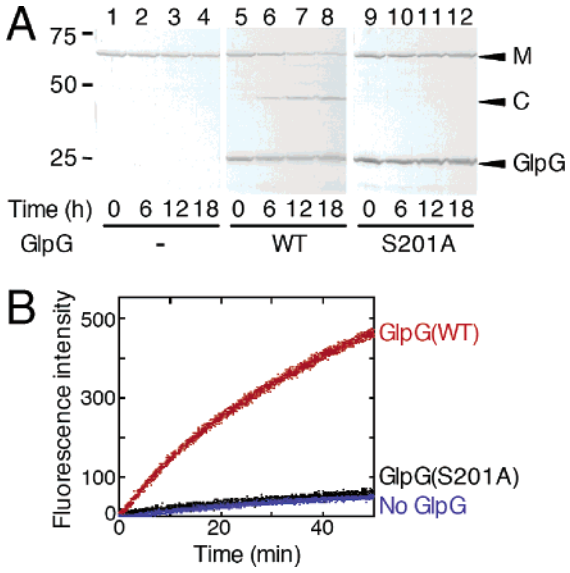

FIGURE 4: Demonstration of the proteolytic activity of GlpG in vitro. (A) Cleavage of the Bla−LacYTM2−MBP-His_6 protein by GlpG-His_6-Myc. Purified Bla−LacYTM2−MBP-His_6 protein (0.5 μM) was mixed with GlpG-His_6-Myc (2.5 μM, lanes 5−8), GlpG-(S201A)-His_6-Myc (2.5 μM, lanes 9−12), or buffer alone (lanes 1−4) and incubated at 37 °C. The reaction mixtures were sampled at the indicated time points and subjected to SDS−PAGE and CBB staining. Molecular size marker positions (kilodaltons) are shown at left. (B) Casein degradation activity of GlpG. BODIPY-casein (25 μg/mL) was mixed with GlpG-His_6-Myc (12.5 μg/mL, red), GlpG(S201A)-His_6-Myc (12.5 μg/mL, black), or buffer alone (blue) at 37 °C, and the BODIPY fluorescence was followed during incubation at 37 °C as described in Experimental Procedures.

guishable from that of the in vivo-generated C fragment (Figure 4A, lanes 5−8). This fragment indeed reacted with anti-MBP upon immunoblotting (data not shown). In the reaction mixture described above, we also detected the generation of the N fragment of the expected size by anti-Bla immunoblotting (data not shown), although it was not revealed by CBB staining in the Figure 4A experiment due to the coincidental electrophoretic mobilities of this fragment and GlpG-His_6-Myc. The "active site" variant, GlpG-(S201A)-His_6-Myc, was inactive in catalyzing cleavage of the model substrate (Figure 4A, lanes 9−12).

We also found that purified GlpG, but not the S201A variant, significantly degraded a hydrophilic soluble protein, BODIPY-casein, whose proteolytic degradation can be monitored by the increase in fluorescence (Figure 4B). Incubation of BODIPY-casein with GlpG-His_6-Myc resulted in the significant and continuous increase of fluorescence over the course of 50 min. No significant fluorescence change was observed when GlpG(S201A)-His_6-Myc was used instead of wild-type GlpG (Figure 4B). These results establish that GlpG has an endoproteolytic activity for cleaving the model membrane protein in vivo and in vitro and for cleaving casein in vitro.

Identification of the Cleavage Site. The in vivo-generated C fragment of the Bla−LacYTM2−MBP-His_6 protein was affinity purified by Ni−NTA chromatography (Figure 3A, lane 7). Its N-terminal amino acid sequence was determined to be DTGII, which is found within the LacY-derived region immediately N-terminal to the predicted TM2 sequence (see Figure 2A). The in vitro-generated C fragment was also sequenced, yielding the same N-terminal sequence, DTGII. Assuming that there was no exoproteolysis in the in vitro system with the purified components, GlpG should cleave the Ser−Asp bond of the model substrate protein (Figure 2A). Contrary to the expectation that GlpG acts against the membrane-embedded polypeptide region, the above analysis suggested that GlpG recognizes a substrate region that is highly hydrophilic and even charged.

Requirements and Specificity of the Membrane Protein Cleavage by GlpG. To study what features of a membrane protein are important for the cleavage by GlpG, we examined two other constructs, Bla−LacYTM2 and MBP−LacYTM2, for their cleavage by GlpG. Bla−LacYTM2 without the cytoplasmic MBP domain and MBP−LacYTM2 having a periplasmic MBP domain were both found to be cleaved GlpG-dependently at 37 °C (Figure 5B) and 25 °C (data not shown). These results suggest that neither of the soluble domains, Bla and MBP, is specifically required for GlpG-catalyzed proteolysis.

We then replaced the LacYTM2 sequence of Bla−LacYTM2−MBP-His_6 with the sixth transmembrane region of LacY (LacYTM6), the sixth transmembrane region of SecY (SecYTM6), the transmembrane region of Spitz (SpitzTM), or 20 consecutive leucine residues (L20). All of these TM variants accumulated as the full-length products in both the *glpG*$^+$ and Δ*glpG* strains, indicating that they are no longer susceptible to GlpG cleavage (Figure 5C). Taken together, these results suggest that GlpG specifically recognizes the LacYTM2 sequence that is arranged in the type I configuration in the membrane for its cleavage.

DISCUSSION

In this study, we established the in vivo and in vitro assay systems for the proteolytic function of GlpG, an *E. coli* rhomboid protein. A Bla−LacYTM2−MBP-His_6 model membrane protein underwent a GlpG-dependent cleavage in *E. coli* cells. We also demonstrated directly that GlpG is able to cleave this model protein, using the purified preparations of the enzyme and the substrate. Very recently, Lemberg et al. (*13*) and Urban and Wolfe (*12*) described proteolytic activities of purified GlpG and other rhomboid proteins. Our and their results show that the GlpG protease does not require other proteins or small molecule cofactors as essential catalytic components.

Rhomboid proteins have three conserved residues (Ser, His, and Asn) that have been proposed to form a serine protease active site (catalytic triad). For several rhomboid proteins, including GlpG, mutational alterations of these residues compromise their functions in cultured eukaryotic cells (*4*). However, an alanine substitution for the conserved Asn residue of *B. subtilis* YqgP caused only a weak effect on its in vivo and in vitro activities (*4*, *13*). Our results also indicate that the conserved Asn residue (Asn154) is not essential, in contrast to the other two conserved residues (Ser201 and His254), for the proteolytic activity of GlpG in *E. coli* cells. However, it remains to be clarified why the mutational alteration of Asn154 severely inhibited the cleavage of Gurken by GlpG in cultured eukaryotic cells (*4*), and whether the proteolytic active sites of prokaryotic rhomboids are composed of a Ser-His dyad.

We have shown that in vivo cleavage of the model protein by GlpG required its membrane assembly in a type I

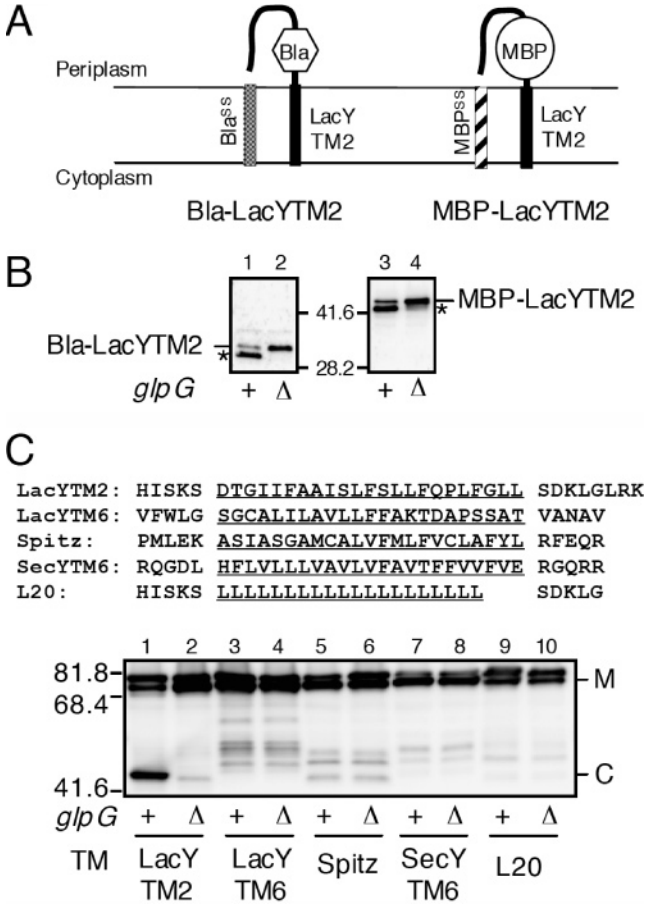

FIGURE 5: Requirements and specificity of the model membrane protein cleavage by GlpG. (A) Schematic representation of Bla−LacYTM2 and MBP−LacYTM2 proteins. MBP^{SS} indicates the signal sequence of MBP. (B) GlpG-dependent cleavage of Bla−LacYTM2 and MBP−LacYTM2 proteins. Cells of CU141 (*glpG*$^+$)/pGW78 (Bla−LacYTM2) (lane 1), GW220 (*glpG*::*cat*)/pGW78 (lane 2), GW170/pGW73 (MBP−LacYTM2) (lane 3), and GW221/pGW73 (lane 4) were grown at 37 °C in L medium and exposed to 1 mM IPTG and 1 mM cAMP for 1 h. Total cellular proteins were then subjected to SDS−PAGE separation and anti-Bla (lanes 1 and 2) or anti-MBP (lanes 3 and 4) immunoblotting. Asterisks indicate the N-terminal fragments of Bla−LacYTM2 (lane 1) and MBP−LacYTM2 (lane 3) that were generated by GlpG-dependent cleavage. Molecular size marker positions (kilodaltons) are shown between lanes 2 and 3. (C) Inability of GlpG to cleave derivatives of the model protein with other transmembrane sequences. Cells of GW170 (lanes 1, 3, 5, 7, and 9) and GW221 (lanes 2, 4, 6, 8, and 10) were transformed with pGW93 (Bla−LacYTM2−MBP-His_6, lanes 1 and 2), pSTD989 (Bla−LacYTM6−MBP-His_6, lanes 3 and 4), pSTD991 (Bla−SpitzTM−MBP-His_6, lanes 5 and 6), pSTD990 (Bla−SecYTM6−MBP-His_6, lanes 7 and 8), or pSTD992 (Bla−L20−MBP-His_6, lanes 9 and 10). Cells were grown and total cellular proteins were analyzed by anti-MBP immunoblotting as described above. Molecular size marker positions (kilodaltons) are shown at left. Amino acid sequences of the transmembrane regions (possible transmembrane regions are underlined) that are used are shown in the top part. The five amino acid residues franking the L20 sequence are derived from the corresponding regions of LacYTM2. Note that addition of NaN_3 to cells before induction resulted in accumulation of precursor forms of the respective model substrates, suggesting that they are correctly assembled into the membrane under a normal condition (data not shown).

orientation. The LacY TM2 sequence is specific in that it is recognized by GlpG when present as a part of the model substrate. Although our model substrate was an artificially constructed chimeric protein, no other TM-derived sequences conferred the GlpG sensitivity. We believe that proteolysis of the model protein by GlpG reflects its essential substrate specificity.

From mutational analysis of Spitz, a substrate of *Drosophila* rhomboid-1, Urban and Freeman (*11*) identified the "substrate motif" in its lumen−membrane interface region, as a determinant of the substrate specificity of this rhomboid protease. Although the exact cleavage site in Spitz (or those in any other rhomboid substrates) is unknown, it was suggested to be located within the substrate motif. In the work presented here, we identified the GlpG cleavage site in the model substrate, Bla−LacYTM2−MBP, by the N-terminal amino acid sequence analysis of the in vitro cleavage product, which agreed with the in vivo product. Our results show that the in vivo and in vitro cleavages occur at the same position within the LacY-derived sequence. Although the amino acid sequence around the cleavage site in this model protein does not obviously conform to the substrate motif and does not have the GA motif (*11*) known to be important for the cleavage of Spitz, its overall sequence property is similar to that of the substrate motif at least in its hydrophilic and helix-destabilizing nature. However, the substrate motif does not appear to be the sole determinant of the cleavage by rhomboids since some substrates such as Gurken do not contain the substrate motif.

The cytoplasmic domain of thrombomodulin is crucial for its cleavage by mammalian RHBDL2 (*23*). We found that neither a deletion of the cytoplasmic MBP domain nor a replacement of the N-terminal Bla domain with MBP in the model substrate affected its cleavage by GlpG in vivo. At least for these model substrates, GlpG does not require a specific sequence arrangement of the substrate soluble domains for proteolysis. Our results showed that GlpG efficiently cleaved the LacYTM2 sequence in vivo, whereas little or essentially no cleavage was observed for several other transmembrane sequences, including SpitzTM, which is a good substrate for *Drosophila* rhomboids. Urban and Freeman (*11*) showed that GlpG can cleave Spitz by recognizing its substrate motif in cultured mammalian cells, although the cleavage efficiency was extremely low. The observed inability of GlpG to cleave SpitzTM in an *E. coli* cell might partly be able to be ascribed to the difference in membrane environments between *E. coli* and mammalian cells; it was shown that *E. coli* lipids severely inhibited the proteolytic activity of GlpG against a model substrate having a Spitz-derived substrate motif in vitro (*12*). Although rhomboids are considered to be highly specific proteases, they may act against a certain spectrum of sequences, and each rhomboid enzyme may have some unique preference with respect to the proteolytic target sequences. Clearly, further experiments are needed to clarify the feature of amino acid sequence that GlpG recognizes for proteolysis. Given that GlpG could recognize more diverse sequences than expected, it might be difficult to identify its physiological substrates solely on the basis of sequence information.

An amino acid sequence (Ser-Lys-Ser-Asp-Thr-Gly) surrounding the GlpG cleavage site in the Bla−LacYTM2−MBP-His_6 protein has high local hydrophilicity; it even contains two charged residues at positions P2 (Lys) and P1′ (Asp). Although the mode of the GlpG action we revealed in this work might not be regarded as exclusive, cleavage of a hydrophilic sequence at a membrane−periplasm interface region should be one intrinsic reactivity of GlpG. We

found that solubilized GlpG exhibited a weak but significant activity for degrading a soluble protein, fluorescence dye-labeled casein, in vitro. Although the GlpG cleavage sites in casein are unknown, this finding seems to be consistent with the observed ability of GlpG to cleave a hydrophilic sequence. However, it cannot be concluded that GlpG can cleave a soluble protein in vivo; under solubilized in vitro conditions, some unstructured soluble proteins such as casein could gain artificial access to the active site of GlpG.

In the native LacY protein, the above SKSDTG sequence is located at the interface between the first periplasmic loop and the second transmembrane helix (*24*). Without structural information, it is difficult to define the membrane-embedded residues of the Bla−LacYTM2−MBP-His_6 protein. Nevertheless, the hydrophilic nature of the cleavage site region in the model protein raises the possibility that the cleavage site is exposed to the periplasm.

On the other hand, the above possibility should be contrasted with the experimentally determined topology of GlpG, in which the proposed proteolytic active site residues (Ser201 and His254) are located within the regions identified as membrane-spanning regions, although whether they are actually embedded in the membrane is difficult to address at this point without structural or additional biochemical information. Does GlpG have to overcome any topological segregation between its active site and the cleavage point on the substrate? Although further detailed studies, including structural analysis, are needed to answer this question, one highly speculative but intriguing possibility might be that GlpG forms an aqueous microenvironment, in which a hydrophilic sequence around the cleavage site of the membrane-bound substrate might be accommodated for their cleavage. Our preliminary results suggest that GlpG forms a homooligomer in the membrane as well as after purification in detergent (unpublished data). The possible oligomeric structure of GlpG could contribute to the hypothetical aqueous microenvironment in the membrane.

We designed our substrate protein solely as a single spanning membrane protein of type I orientation composed of some well-characterized protein segments. It is surprising that this rather fortuitous construct turned out to be a substrate of GlpG, both in vivo and in vitro. This experimental system could be useful for characterization of basic activities of GlpG, if not its regulatory aspects. In our characterization of another "RIP" protease, RseP, we encountered the broad substrate specificity of this protease despite its involvement in the strictly controlled stress response pathway in vivo (*19*). Although the actual cellular function of GlpG is unknown, these membrane proteases might be equipped with a broader than expected hydrolytic reactivity that is integrated into a specific context of regulation.

ACKNOWLEDGMENT

We thank H. Mori and K. Inaba for helpful suggestions and stimulating discussion and K. Mochizuki, M. Sano, Y. Yoshikaie, and T. Adachi for technical support.

REFERENCES

1. Weihofen, A., and Martoglio, B. (2003) Intramembrane-cleaving proteases: Controlled liberation of proteins and bioactive peptides, *Trends Cell Biol. 13*, 71−8.
2. Wolfe, M. S., and Kopan, R. (2004) Intramembrane proteolysis: Theme and variations, *Science 305*, 1119−23.
3. Urban, S., Lee, J. R., and Freeman, M. (2001) *Drosophila* rhomboid-1 defines a family of putative intramembrane serine proteases, *Cell 107*, 173−82.
4. Urban, S., Schlieper, D., and Freeman, M. (2002) Conservation of intramembrane proteolytic activity and substrate specificity in prokaryotic and eukaryotic rhomboids, *Curr. Biol. 12*, 1507−12.
5. Koonin, E. V., Makarova, K. S., Rogozin, I. B., Davidovic, L., Letellier, M. C., and Pellegrini, L. (2003) The rhomboids: A nearly ubiquitous family of intramembrane serine proteases that probably evolved by multiple ancient horizontal gene transfers, *Genome Biol. 4*, R19.
6. Urban, S., Lee, J. R., and Freeman, M. (2002) A family of rhomboid intramembrane proteases activates all *Drosophila* membrane-tethered EGF ligands, *EMBO J. 21*, 4277−86.
7. McQuibban, G. A., Saurya, S., and Freeman, M. (2003) Mitochondrial membrane remodelling regulated by a conserved rhomboid protease, *Nature 423*, 537−41.
8. Herlan, M., Vogel, F., Bornhovd, C., Neupert, W., and Reichert, A. S. (2003) Processing of Mgm1 by the rhomboid-type protease Pcp1 is required for maintenance of mitochondrial morphology and of mitochondrial DNA, *J. Biol. Chem. 278*, 27781−8.
9. Rather, P. N., Ding, X., Baca-DeLancey, R. R., and Siddiqui, S. (1999) *Providencia stuartii* genes activated by cell-to-cell signaling and identification of a gene required for production or activity of an extracellular factor, *J. Bacteriol. 181*, 7185−91.
10. Gallio, M., Sturgill, G., Rather, P., and Kylsten, P. (2002) A conserved mechanism for extracellular signaling in eukaryotes and prokaryotes, *Proc. Natl. Acad. Sci. U.S.A. 99*, 12208−13.
11. Urban, S., and Freeman, M. (2003) Substrate specificity of rhomboid intramembrane proteases is governed by helix-breaking residues in the substrate transmembrane domain, *Mol. Cell 11*, 1425−34.
12. Urban, S., and Wolfe, M. S. (2005) Reconstitution of intramembrane proteolysis in vitro reveals that pure rhomboid is sufficient for catalysis and specificity, *Proc. Natl. Acad. Sci. U.S.A. 102*, 1883−8.
13. Lemberg, M. K., Menendez, J., Misik, A., Garcia, M., Koth, C. M., and Freeman, M. (2005) Mechanism of intramembrane proteolysis investigated with purified rhomboid proteases, *EMBO J. 24*, 464−72.
14. Kanehara, K., Ito, K., and Akiyama, Y. (2002) YaeL (EcfE) activates the σ^E pathway of stress response through a site-2 cleavage of anti-σ^E, RseA, *Genes Dev. 16*, 2147−55.
15. Shimohata, N., Chiba, S., Saikawa, N., Ito, K., and Akiyama, Y. (2002) The Cpx stress response system of *Escherichia coli* senses plasma membrane proteins and controls HtpX, a membrane protease with a cytosolic active site, *Genes Cells 7*, 653−62.
16. Davis, R. W., Botstein, D., and Roth, J. R. (1980) *Advanced Bacterial Genetics*, Cold Spring Harbor Laboratory Press, Plainview, NY.
17. Miller, J. H. (1972) *Experiments in Molecular Genetics*, Cold Spring Harbor Laboratory Press, Plainview, NY.
18. Kanehara, K., Akiyama, Y., and Ito, K. (2001) Characterization of the *yaeL* gene product and its S2P-protease motifs in *Escherichia coli*, *Gene 281*, 71−9.
19. Akiyama, Y., Kanehara, K., and Ito, K. (2004) RseP (YaeL), an *Escherichia coli* RIP protease, cleaves transmembrane sequences, *EMBO J. 23*, 4434−42.
20. Kihara, A., Akiyama, Y., and Ito, K. (1996) A protease complex in the *Escherichia coli* plasma membrane: HflKC (HflA) forms a complex with FtsH (HflB), regulating its proteolytic activity against SecY, *EMBO J. 15*, 6122−31.
21. Prinz, W. A., and Beckwith, J. (1994) Gene fusion analysis of membrane protein topology: A direct comparison of alkaline phosphatase and β-lactamase fusions, *J. Bacteriol. 176*, 6410−3.
22. Daley, D. O., Rapp, M., Granseth, E., Melen, K., Drew, D., and von Heijne, G. (2005) Global topology analysis of the *Escherichia coli* inner membrane proteome, *Science 308*, 1321−3.
23. Lohi, O., Urban, S., and Freeman, M. (2004) Diverse substrate recognition mechanisms for rhomboids: Thrombomodulin is cleaved by mammalian rhomboids, *Curr. Biol. 14*, 236−41.
24. Abramson, J., Smirnova, I., Kasho, V., Verner, G., Kaback, H. R., and Iwata, S. (2003) Structure and mechanism of the lactose permease of *Escherichia coli*, *Science 301*, 610−5.

25. Kihara, A., Akiyama, Y., and Ito, K. (1995) FtsH is required for proteolytic elimination of uncomplexed forms of SecY, an essential protein translocase subunit, *Proc. Natl. Acad. Sci. U.S.A. 92*, 4532−6.
26. Silhavy, T. J., Berman, M. L., and Enquist, L. W. (1984) *Experiments with Gene Fusions*, Cold Spring Harbor Laboratory Press, Plainview, NY.
27. Akiyama, Y., Ogura, T., and Ito, K. (1994) Involvement of FtsH in protein assembly into and through the membrane I. Mutations that reduce retention efficiency of a cytoplasmic reporter, *J. Biol. Chem. 269*, 5218−24.
28. Akiyama, Y., and Ito, K. (1990) SecY protein, a membrane-embedded secretion factor of *E. coli*, is cleaved by the OmpT protease *in vitro*, *Biochem. Biophys. Res. Commun. 167*, 711−5.
29. Inaba, K., and Ito, K. (2002) Paradoxical redox properties of DsbB and DsbA in the protein disulfide-introducing reaction cascade, *EMBO J. 21*, 2646−54.
30. Strauch, K. L., Johnson, K., and Beckwith, J. (1989) Characterization of degP, a gene required for proteolysis in the cell envelope and essential for growth of *Escherichia coli* at high temperature, *J. Bacteriol. 171*, 2689−96.
31. Takeshita, S., Sato, M., Toba, M., Masahashi, W., and Hashimoto-Gotoh, T. (1987) High-copy-number and low-copy-number plasmid vectors for *lacZ* α-complementation and chloramphenicol- or kanamycin-resistance selection, *Gene 61*, 63−74.
32. Mayer, M. P. (1995) A new set of useful cloning and expression vectors derived from pBlueScript, *Gene 163*, 41−6.
33. Kanehara, K., Ito, K., and Akiyama, Y. (2003) YaeL proteolysis of RseA is controlled by the PDZ domain of YaeL and a Gln-rich region of RseA, *EMBO J. 22*, 6389−98.
34. Akiyama, Y., Yoshihisa, T., and Ito, K. (1995) FtsH, a membrane-bound ATPase, forms a complex in the cytoplasmic membrane of *Escherichia coli*, *J. Biol. Chem. 270*, 23485−90.
35. Kyte, J., and Doolittle, R. F. (1982) A simple method for displaying the hydropathic character of a protein, *J. Mol. Biol. 157*, 105−32.
36. Hirokawa, T., Boon-Chieng, S., and Mitaku, S. (1998) SOSUI: Classification and secondary structure prediction system for membrane proteins, *Bioinformatics 14*, 378−9.

BI051363K